

## Supplementary Information

---

### **Azo-Functionalised Metal-Organic Framework for Charge Storage in Sodium-ion Batteries**

*Aamod V. Desai,<sup>a,b</sup> Valerie R. Seymour,<sup>b,c</sup> Romy Ettliger,<sup>a</sup> Atin Pramanik,<sup>a</sup> Alexis G. Manche,<sup>a,b</sup> Daniel N. Rainer,<sup>a</sup> Paul S. Wheatley,<sup>a</sup> John M. Griffin,<sup>b,c</sup> Russell E. Morris<sup>\*,a,b</sup> and A. Robert Armstrong<sup>\*,a,b</sup>*

a - EastChem School of Chemistry, University of St Andrews, North Haugh, St Andrews KY16 9ST, United Kingdom.

b - The Faraday Institution, Quad One, Harwell Science and Innovation Campus, Didcot, OX11 0RA, United Kingdom.

c - Department of Chemistry, Lancaster University, Lancaster LA1 4YB, UK.

Email: [rem1@st-andrews.ac.uk](mailto:rem1@st-andrews.ac.uk) ; [ara@st-andrews.ac.uk](mailto:ara@st-andrews.ac.uk)

---

## Experimental Details

### *Materials*

The reagents – Zirconium chloride ( $ZrCl_4$ ; Sigma Aldrich), azobenzene-4,4'-dicarboxylic acid ( $H_2abdc$ ; TCI Chemicals), L-proline (TCI Chemicals), hydrochloric acid (HCl; Fisher Chemical), N,N'-dimethylformamide (DMF; Fisher Chemical), methanol (MeOH; Fisher Chemical), dichloromethane (DCM; Fisher Chemical), dimethyl carbonate (DMC; Sigma Aldrich) were obtained commercially and used as received. The chemicals for electrochemical studies – Super C65 (Imerys Graphite & Carbon), sodium carboxymethyl cellulose (degree of substitution 1.2, Sigma Aldrich) were also obtained from commercial sources.

### *Synthesis of UiO-abdc*

UiO-abdc was prepared following a previously reported procedure.<sup>1</sup> To a solution of  $ZrCl_4$  (0.2098 g, 0.9 mmol) in DMF (10 mL), concentrated HCl (0.08 mL) was added and sonicated for 5 minutes. L-proline (0.518 g, 4.5 mmol) was added to this solution as a solid and the mixture sonicated for a further 5 minutes. Subsequently, the ligand -  $H_2abdc$  (0.2432 g, 0.9 mmol) and DMF (10 mL) was added, and the mixture sonicated for 5 minutes. This was placed in a glass jar with screw cap and heated at 120 °C for 24 hours. Upon cooling, an orange colour precipitate was obtained which was filtered off and washed with DMF (2 × 30 mL). The powder was subsequently stirred in MeOH for 6 hours, with the solvent replaced every 2 hours. The solid was then suspended in DCM overnight and filtered off and left to dry at 80 °C for 8 hours.

### *Structural Characterization*

Powder X-ray diffraction (PXRD) patterns were recorded on STOE STADIP diffractometer using  $Mo K_{\alpha 1}$  radiation at room temperature from 1.5-27.5° ( $2\theta$ ) in capillary Debye-Scherrer mode. Thermogravimetric analysis (TGA) was recorded in air on NETZSCH STA 449F5 from room temperature to 700 °C, with heating rate of 5 °C per minute. IR spectroscopy was carried out using Shimadzu IR affinity-1 FTIR spectrophotometer in transmittance mode from 400-4000  $cm^{-1}$ . SEM images were collected using a JEOL JSM-IT800 microscope. The powdered samples were placed on copper tape. Raman spectra were recorded on The Renishaw In-Via Qontor Raman microscope using a laser excitation of 532 nm.

### *Experimental NMR*

Solid-State NMR spectra were performed on Bruker Avance III HD spectrometers operating at magnetic field strengths of 9.4 and 16.4 T. For the *ex situ* studies, the powders were packed into NMR rotors in an argon glovebox.  $^{23}Na$  NMR spectra were recorded using high power  $^1H$

decoupling.  $^{23}\text{Na}$  NMR spectra are referenced relative to a solid reference of NaCl (7.2 ppm). Spectra are the sum of 432 transients separated by a recycle interval of 1 s.  $^{13}\text{C}$  NMR spectra are referenced relative to tetramethylsilane using *L*-alanine ( $\text{CH}_3$ , 20.5 ppm) as a secondary reference.  $^1\text{H}$  NMR spectra are also referenced using *L*-alanine ( $\text{NH}_3$ , 8.5 ppm).  $^{13}\text{C}$  NMR spectra were recorded at a magic-angle spinning (MAS) rate of between 12.5 and 15 kHz using cross polarisation (CP) to transfer magnetisation from  $^1\text{H}$  with a contact time of between 1 and 5 ms. The CP pulse was ramped linearly from 70% to 100% power.  $^1\text{H}$  heteronuclear decoupling using two-pulse phase modulation (TPPM)<sup>2</sup> with a pulse length of 4.8 s and a radiofrequency field strength of 100 kHz was applied during acquisition. Spectra are the sum of between 704 and 25680 transients separated by a recycle interval of between 5 and 10 s.  $^1\text{H}$  NMR spectra were recorded using a DEPTH pulse sequence, with a MAS rate of between 12.5 and 15 kHz. Spectra are the sum of between 64 and 6400 transients separated by a recycle interval of between 5 and 20 s.

#### *Gas adsorption*

BET-specific surface area determination from  $\text{N}_2$  isotherms was carried according to the Rouquerol theory<sup>3</sup> using the Microactive Software Kit v4.03.04. Data was recorded on a Micromeritics ASAP 2020 Accelerated Surface Area and Porosity System. Sample (~100 mg) was added to a frit tube and activated in vacuo (120 °C,  $\sim 3 \times 10^{-5}$  mbar, 12 h) prior to the measurement.

#### *Electrochemical Characterization*

The working electrodes were prepared by mixing the MOF powder (60%), conductive carbon (Super C65, 30%) and carboxymethyl cellulose (CMC, 10%) as the binder. The slurry was prepared by hand grinding a mixture of the active material and conductive carbon which was added to the binder solution in water and stirred for 3 h. The slurry was cast onto aluminium foil (Advent Research) using a doctor blade and air dried for 2 h. Electrodes were then punched (diameter ~12 mm) and dried overnight in a vacuum oven at 110 °C. The approximate active mass loading was  $1.7 \text{ mg cm}^{-2}$ .

Solid state characterisation (Raman spectra and SEM images) for the dried electrode phase was performed by scraping off the solid mixture from the Al-foil. Coin cells (CR2032) were assembled using sodium metal (Sigma-Aldrich) as the counter electrode, glass fiber separator (Whatman GF/F) and  $\text{NaPF}_6$  in ethylene carbonate (EC) and diethyl carbonate (DEC) (1:1, v/v) (Kishida Chemical) as the electrolyte, in an argon-filled glovebox (MBraun) with oxygen and water content < 1 ppm. Electrochemical studies were performed at 30 °C in a potential window of 0.01-2.5 V (vs  $\text{Na}^+/\text{Na}$ ) on a Biologic BCS-805 modular battery testing system and the data were analysed using BT-Lab software, or on a Neware BTS tester and data

processed using BTSDA software. For all electrochemical studies the calculations were based on the mass of the active material (MOF), except for a cell involving only carbon and binder, where the calculation was based on the mass of the carbon.

The *ex situ* Raman spectral analysis was carried out by stopping the coin cells at specified state of charge and preparing the optical cell (EL-Cell) inside the argon-filled glovebox.<sup>4</sup> For *ex situ* NMR, PXRD and SEM measurements, Swagelok cells with electrode powder of MOF and Super C65 (2:1) was used. These cells were cycled at a current density of 25 mA g<sup>-1</sup> (for NMR) or 10 mA g<sup>-1</sup> (for PXRD and SEM) and disassembled inside the glovebox at the specified state of charge. The recovered solid was rinsed with DMC (3 × 7 mL) and dried under vacuum overnight. For *ex situ* SEM analysis, the samples were prepared inside the argon-filled glovebox by depositing a drop of powdered sample dispersed in DMC onto copper tape. Subsequently, the samples were transferred to the microscope using a transfer vessel to avoid air contact.

#### *DFT calculations*

Density functional theory (DFT) calculations were carried out with hybrid exchange-correlation functional B3LYP. A linker mimicking molecule was used to facilitate the calculations and make the peaks of interest on the theoretical spectra more readable (see Figure S12). The basis sets for C, H, O, N and Na atoms of studied molecules were 6-311+G(d,p),<sup>5</sup> which includes a polarisation function to all five kinds of atoms and a diffuse function to C, N, and H atoms. There is no setting of the symmetric restriction or predefined conformation for optimising. Full geometric optimisation was carried out by using Gaussian 16 package.

The Raman spectra of the test molecule mimicking the Zr(IV)-based MOF (see Figure S12) were calculated by DFT simulations with the basis set of 6-311+G (d,p) for C, H, O, N and Na atoms and carried out with the Gaussian 16 package. The optimised ground state geometry was used to predict Raman spectrum, and a uniform scaling factor was set to 0.965.

## Figures

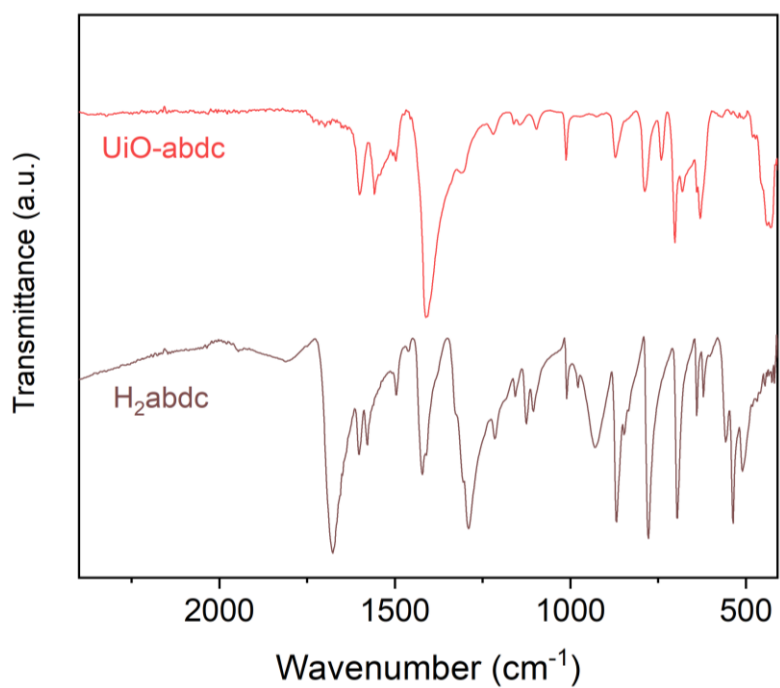


**Figure S1.** FT-IR spectra for ligand (H<sub>2</sub>abdc) and UiO-abdc.

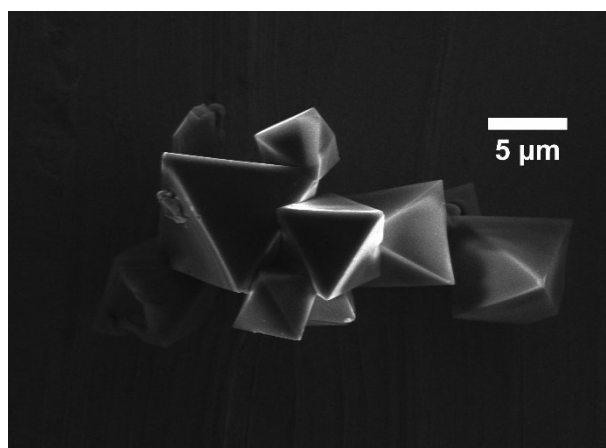


**Figure S2.** SEM image for as-synthesised phase of UiO-abdc.

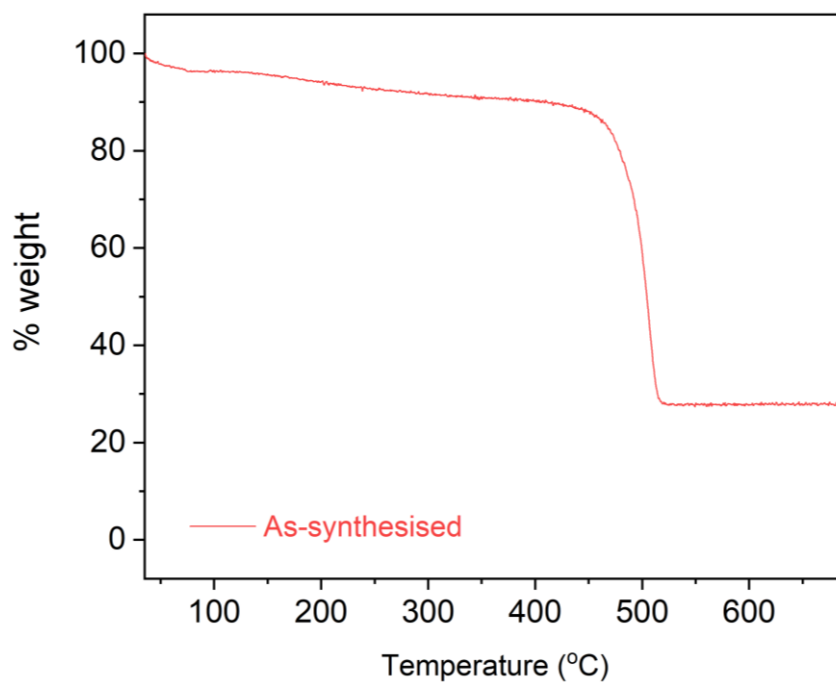


**Figure S3.** TGA profile for UiO-abdc.

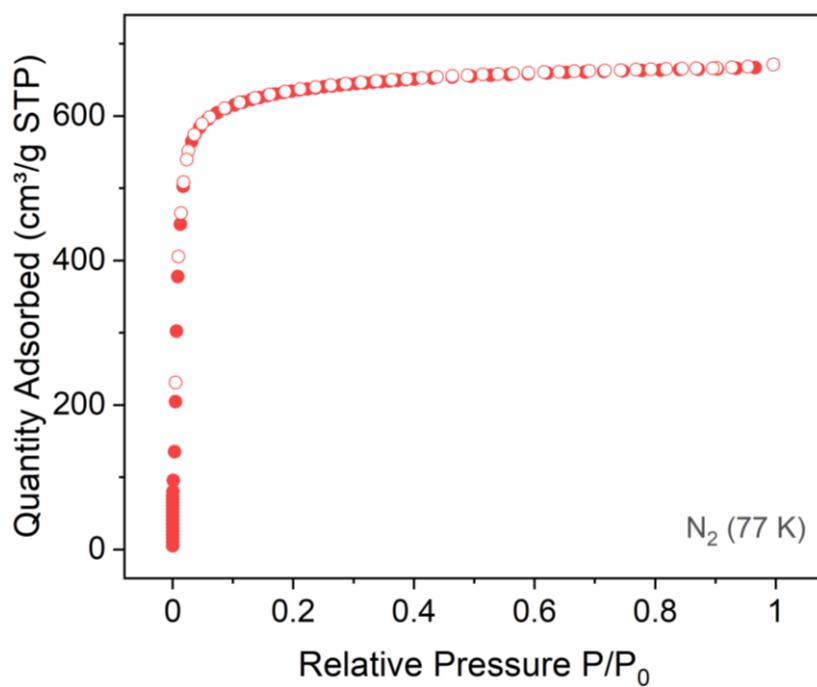


**Figure S4.** Low temperature (77 K) N<sub>2</sub> adsorption isotherm for UiO-abdc. Closed and open symbols represent adsorption and desorption respectively. The BET area was calculated to be 2838±99 m<sup>2</sup>/g.

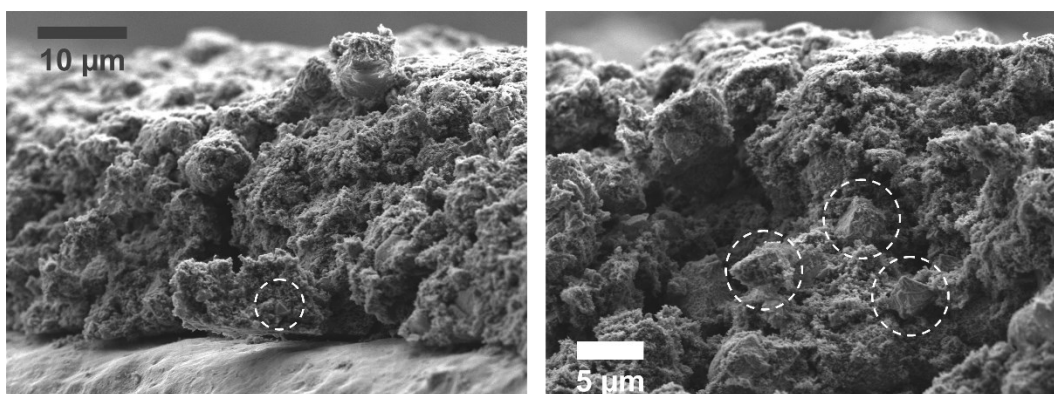


**Figure S5.** SEM images for dried cast electrode of UiO-abdc. Dotted lines showing octahedral shaped crystallites.

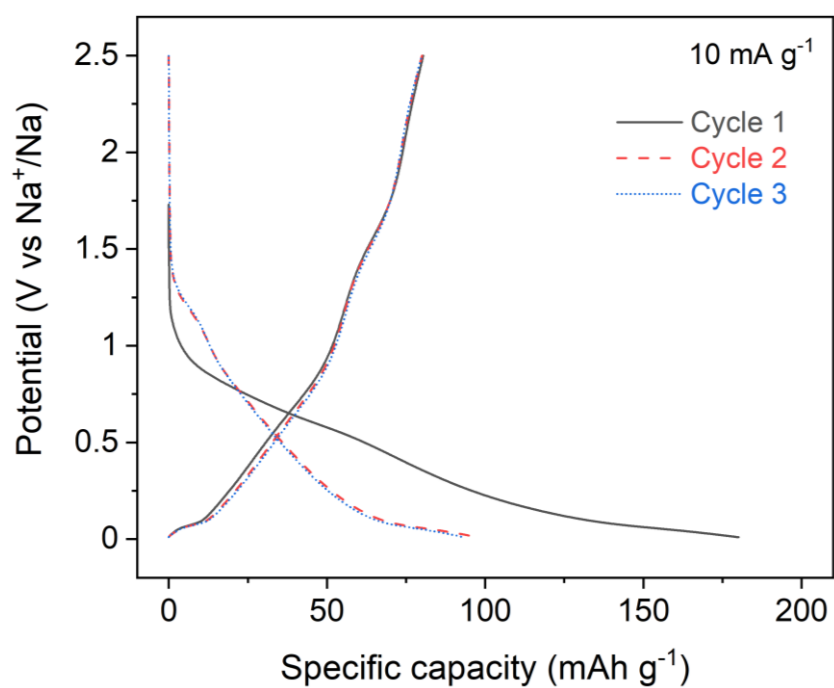


**Figure S6.** Galvanostatic charge/discharge curves for first 3 cycles of UiO-abdc cycled between 0.01-2.5 V at a current rate of 10 mA g<sup>-1</sup>.

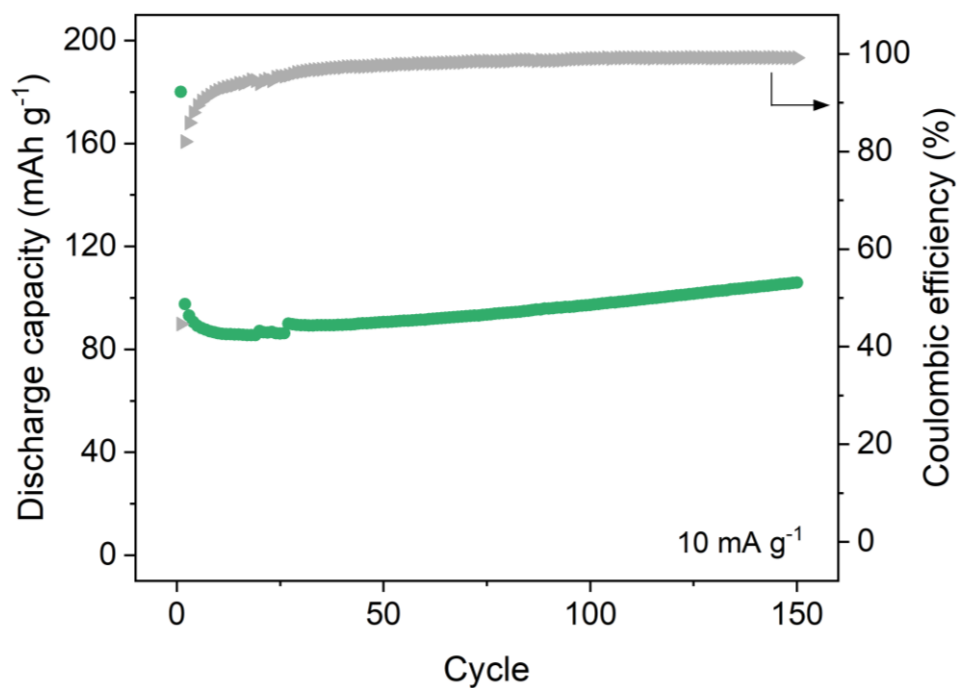


**Figure S7.** Discharge capacities and coulombic efficiencies for UiO-abdc cycled at  $10 \text{ mA g}^{-1}$  between 0.01-2.5 V.

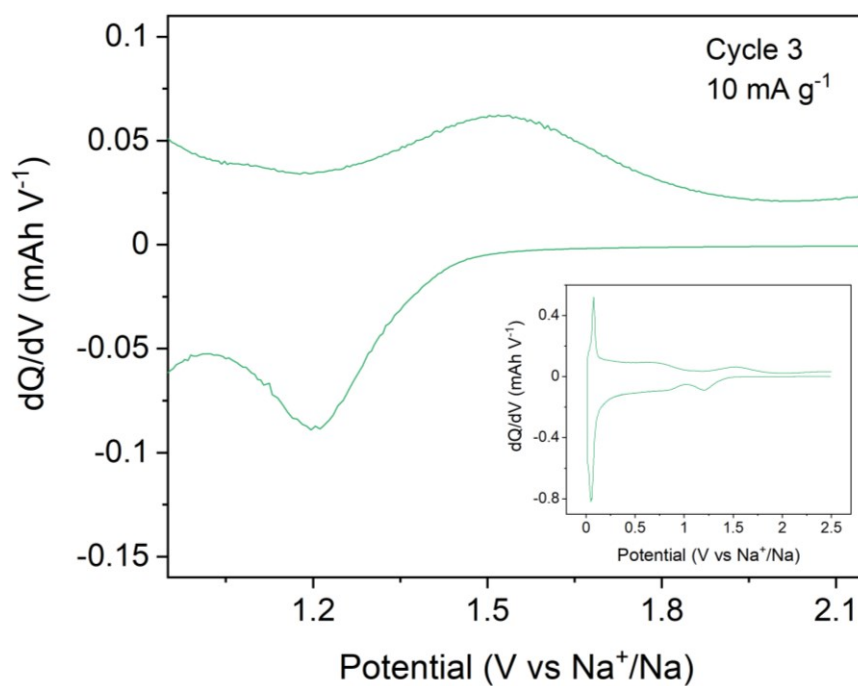


**Figure S8.** Zoomed plot and (inset) full plot of differential capacity for UiO-abdc cycled at  $10 \text{ mA g}^{-1}$  between 0.01-2.5 V.



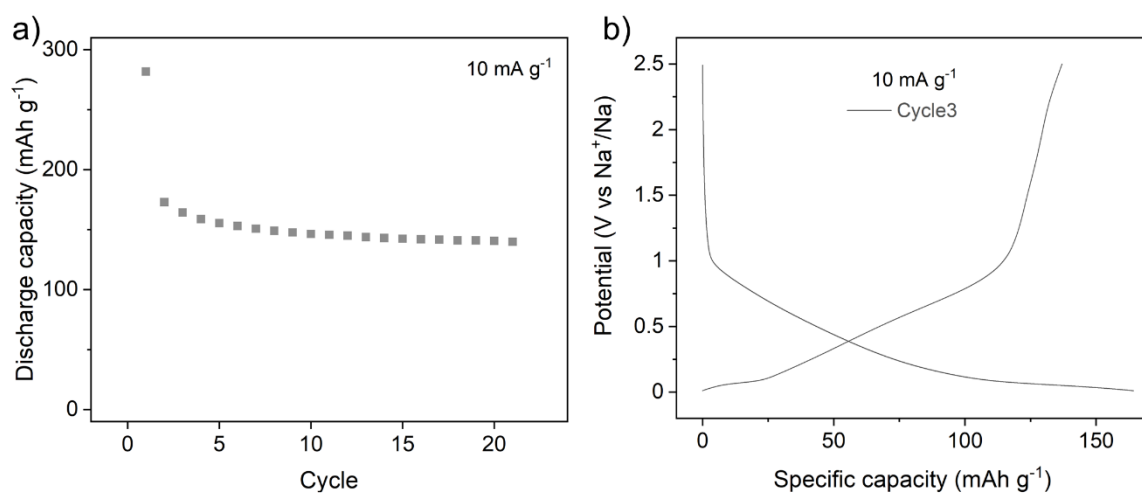


**Figure S9.** a) Discharge capacities for 20 cycles of electrode prepared using conductive carbon (Super C65, 90%) and CMC binder (10%), cycled at  $10 \text{ mA g}^{-1}$  between a potential window of 0.01-2.5 V. Assuming the capacity stabilises at  $\sim 140 \text{ mAh g}^{-1}$ , the maximum contribution of 30% conductive carbon in electrodes of UiO-abdc would be  $\sim 46.66 \text{ mAh g}^{-1}$ . b) Galvanostatic charge/discharge curve for the 3<sup>rd</sup> cycle.

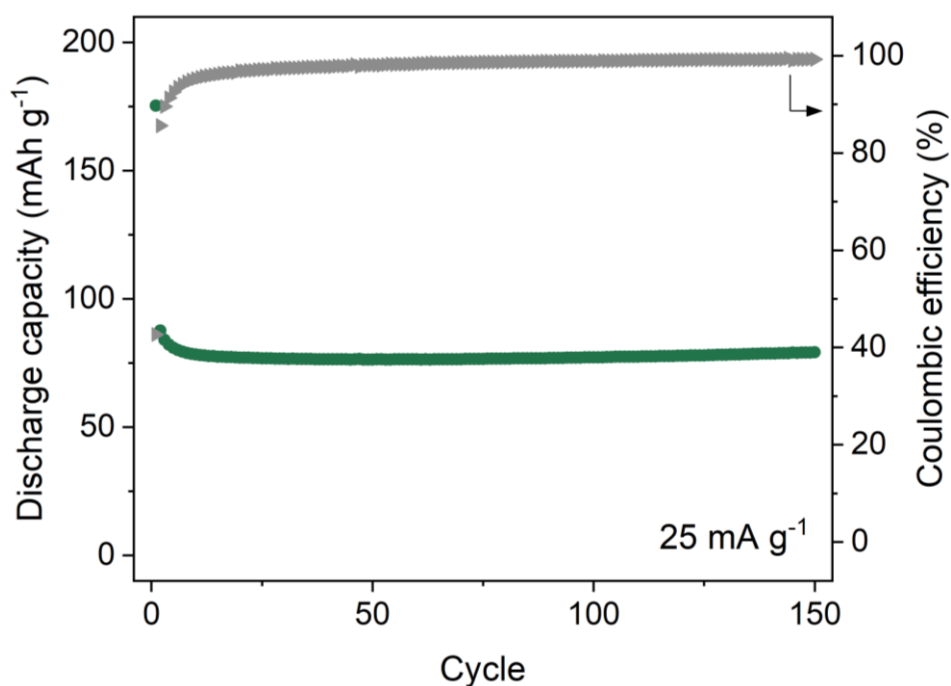


**Figure S10.** Discharge capacities and coulombic efficiencies for UiO-abdc cycled at  $25 \text{ mA g}^{-1}$  between 0.01-2.5 V.

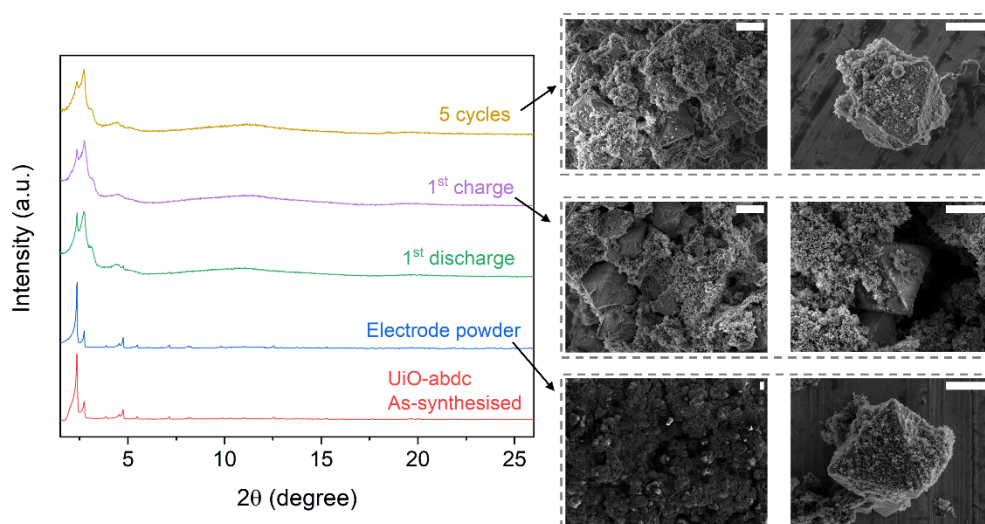


**Figure S11.** PXRD patterns for the electrode powder and for the material after 1<sup>st</sup> discharge (0.01 V), 1<sup>st</sup> charge (2.5 V) and the one obtained after 5 cycles, compared with the pristine phase. Shown alongside are corresponding SEM images for the electrode powder before cycling, material after 1 and 5 cycles (Scale bar 5  $\mu\text{m}$ ).

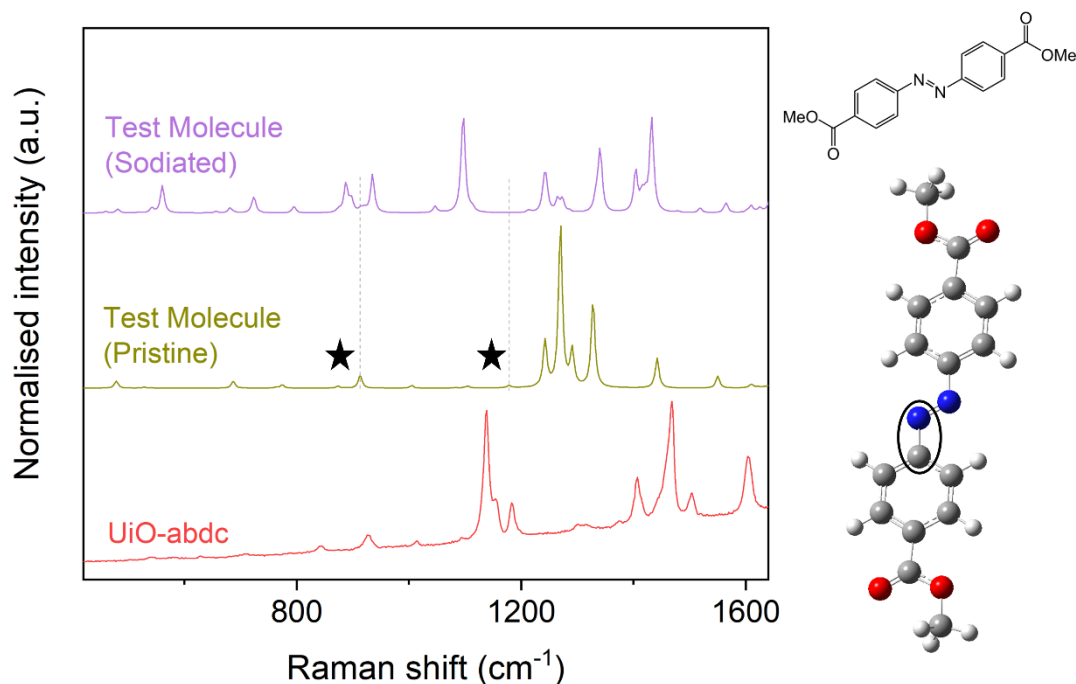


**Figure S12.** Comparison of experimental Raman spectrum from UiO-abdc (red) and DFT estimated Raman pattern for the test molecule (yellow) and the sodiated form (purple). The peaks marked in the simulated spectrum correspond to the vibration modes of the aromatic groups, which are linked to the motion of C-N bond in the linker (shown alongside).

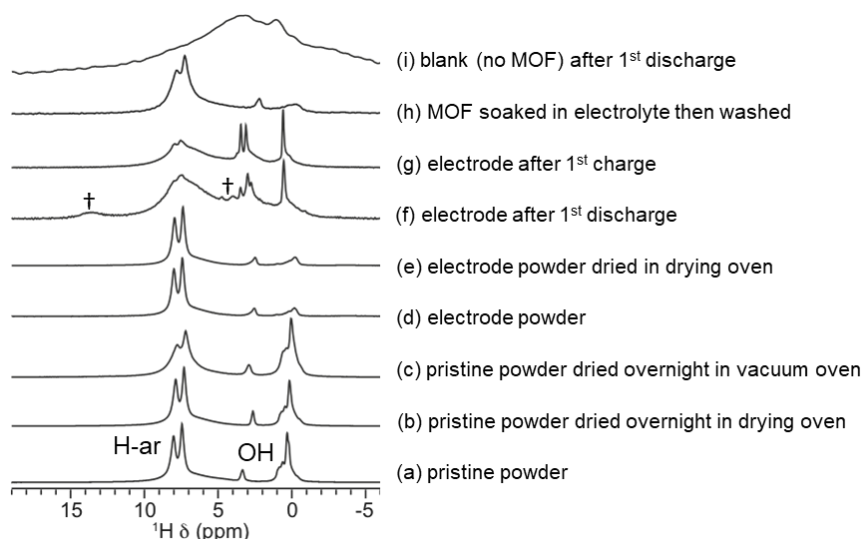


**Figure S13.** <sup>1</sup>H MAS solid-state NMR spectra of pristine UiO-abdc and electrode powders. Spectra (a, b, d-g) were recorded using 15 kHz MAS, 16.4 T and spectra (c, h, i) were recorded using 12.5 kHz MAS at 9.4 T. Resolution of aromatic CH peaks depends on whether it was recorded at 9.4 T or 16.4 T.

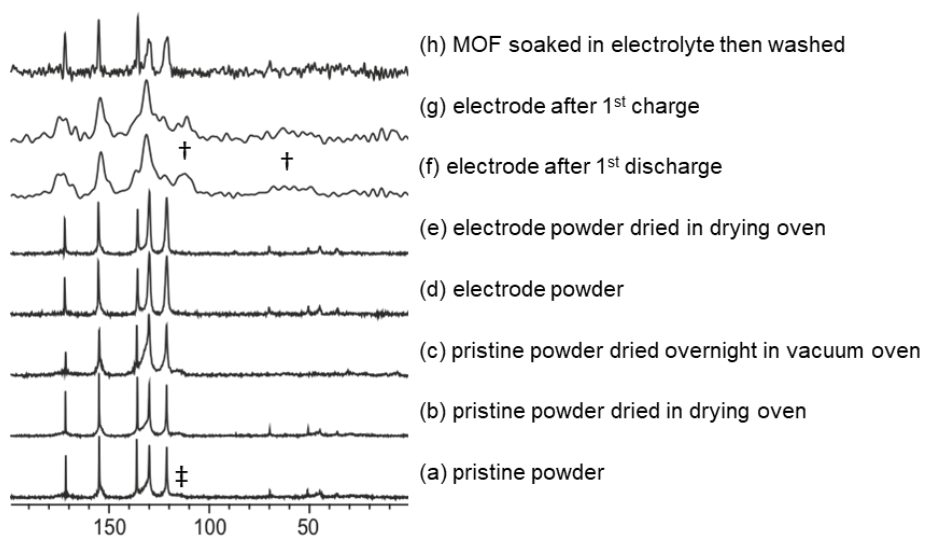


**Figure S14.** <sup>13</sup>C CP MAS solid-state NMR spectra of pristine UiO-abdc and electrode powders. Spectra (a, b, d, e, h) were recorded using 15 kHz MAS, 16.4 T and spectra (c, f, g) were recorded using 12.5 kHz MAS at 9.4 T. ‡ indicates additional peak observed in spectrum of pristine powder, † indicates additional peaks observed in cycled samples.

## References:

- 1 R. J. Marshall, C. L. Hobday, C. F. Murphie, S. L. Griffin, C. A. Morrison, S. A. Moggach and R. S. Forgan, *J. Mater. Chem. A*, 2016, **4**, 6955–6963.
- 2 A. E. Bennett, C. M. Rienstra, M. Auger, K. V Lakshmi and R. G. Griffin, *J. Chem. Phys.*, 1995, **103**, 6951–6958.
- 3 J. Rouquerol, P. Llewellyn and F. Rouquerol, in *Characterization of Porous Solids VII*, eds. P. L. Llewellyn, F. Rodriguez-Reinoso, J. Rouquerol and N. B. T.-S. in S. S. and C. Seaton, Elsevier, 2007, vol. 160, pp. 49–56.
- 4 A. Pramanik, A. G. Manche, R. Clulow, P. Lightfoot and A. R. Armstrong, *Dalt. Trans.*, 2022, **51**, 12467–12475.
- 5 G. Kresse and J. Furthmüller, *Comput. Mater. Sci.*, 1996, **6**, 15–50.